Taylor & Francis
Taylor & Francis Group

RESEARCH PAPER

🔓 OPEN ACCESS   Check for updates

CXCR4 confers stemness and radioresistance in chordoma cells

Chan-Woong Jung*, Jeong-Yub Kim, and Myung-Jin Park 🄳

Division of Radiation Cancer Research, Korea Institute of Radiological and Medical Sciences, Seoul, Korea

ABSTRACT

CXC Chemokine receptor type 4 (CXCR4) is commonly considered a potential marker for cancer stem cells (CSCs). Dedifferentiated-type chordoma (DTC) cells derived from a patient with recurrent chordoma exhibit high CXCR4 expression and demonstrate increased resistance to chemotherapeutic drugs and ionizing radiation (IR) compared to the conventional-type chordoma cell line, U-CH1. However, the precise role of CXCR4 in the stemness and IR resistance of DTC remains unclear. Therefore, this study aims to elucidate the correlation between the expression of CXCR4 and stemness and radioresistance in chordoma. DTC cells expressing CXCR4 (CXCR4+ DTC cells), isolated by magnetic-activated cell sorting, exhibited increased self-renewal activity, tumorigenicity, and IR resistance, accompanied by elevated Sox2 expression. Knockdown of CXCR4 expression using short hairpin RNA, inhibition of CXCR4 signaling with AMD3100, and targeting of STAT3, a downstream effector of CXCR4, with WP1066 in DTC cells significantly diminished their self-renewal ability, tumorigenic potential, IR resistance, and Sox2 expression. Additionally, transfection with a small interfering Sox2 RNA suppressed self-renewal activity, tumorigenicity, and IR resistance in DTC cells, whereas overexpression of CXCR4 reversed these effects in U-CH1 cells. Furthermore, DTC cells infected with shCXCR4 exhibited substantial tumor suppression, and the combination of IR and AMD3100 significantly reduced DTC tumor growth in a mouse xenograft model. These findings underscore the functional significance of CXCR4 as a CSC marker, highlighting its potential as a therapeutic target for malignant chordomas.

Introduction

Chordomas are rare primary bone tumors that develop from notochord remnants.[1,2] They are typically low-grade, poorly differentiated, and locally invasive, possibly because they originate from embryonic notochord remnants in the axial skeleton.[3] Chordomas are classified into three types according to their histological variants: conventional (classic), chondroid, and dedifferentiated. Although rare, chordomas are life-threatening because of their local aggressiveness and progressive nature.[4,5] The standard treatment involves adjuvant radiotherapy after surgery. However, this approach is ineffective, possibly because of recurrence following local invasion.

Recent evidence suggests that cancer stem cells (CSCs) are associated with tumor development, growth, recurrence, and resistance to radiotherapy and chemotherapy.[6,7] Therefore, the efficient elimination of CSCs could significantly improve anticancer treatment strategies. In chordomas, CSCs were first identified by Aydemir et al., who reported CD133-positive and CD15-positive tumor-propagating cells.[8] In a previous study, we established a dedifferentiated chordoma (DTC) cell line from patients with recurrent chordomas.[9] This DTC line displayed increased resistance to anticancer drugs and radiation compared to the conventional-type chordoma cell line, U-CH1, indicating its robust tumorigenic ability. Intriguingly, the molecular expression patterns of DTC were different from those of U-CH1. DTC

exhibited distinct molecular expression patterns, particularly elevated stemness-related factors such as Oct4, c-Myc, CD133, Musashi, FoxM1, and CXC chemokine receptor type 4 (CXCR4).

CXCR4 (CD184) is a seven-transmembrane chemokine receptor typically expressed on immune cells, embryonic stem cells, and mesenchymal stem cells. This receptor plays a significant role in tumor growth, angiogenesis, and metastasis of various cancer cells via CXCR4-SDF1 signaling.[10] While the presence of CXCR4 in hematopoietic malignancies is not surprising because of its vital role in developing these cells, its heightened expression in several cancers compared with that in adjacent normal tissues is noteworthy.[11–13] On the cell surface, CXCR4 is a potential marker of CSCs in diverse cancers such as glioma, prostate cancer, lung cancer, and osteosarcoma.[14–17] Recent studies have suggested that CXCR4 is a surface marker of CSCs in synovial sarcoma-initiating cells.[18] Using a sphere-forming culture method, researchers successfully isolated a subpopulation of CSCs with high CXCR4 expression. These cells exhibited increased tumorigenic activity compared with CXCR4− cells when serially transplanted into NOD/SCID mice, replicating the phenotype observed in the original tumor. High CXCR4 surface expression has also been identified in alveolar rhabdomyosarcoma cells and is correlated with poor patient prognosis.[19] It also serves as a prognostic marker for various soft tissue

---

CONTACT Myung-Jin Park ✉ mjpark@kirams.re.kr 🏢 Division of Radiation Cancer Research, Korea Institute of Radiological and Medical Sciences, 75, Nowon-ro, Nowon-gu, Seoul 01812, Korea

*Present affiliation for Chan-Woong Jung: Department of Life Sciences, Korea University, Seoul, Korea

sarcomas, including malignant peripheral nerve sheath tumors, leiomyosarcoma, liposarcoma, and fibrosarcoma.[20]

The relationship between CXCR4 expression and the CSC phenotype in chordomas remains unexplored. Therefore, the purpose of this study is to elucidate the correlation between CXCR4 expression and stemness as well as radioresistance in chordoma cells. We hypothesized that elevated CXCR4 surface expression is linked to the CSC phenotype in DTC cells. To test this hypothesis, we examined the role of CXCR4 in the self-renewal activity, expression of stemness-related molecules, tumorigenicity, and resistance to ionizing radiation (IR) in DTC and conventional chordoma cells. As a result, the suppression of CXCR4 expression in DTC cells led to a decrease in stemness and increased sensitivity to radiation therapy, whereas overexpression of CXCR4 in the conventional chordoma cell line U-CH1 resulted in increased stemness and radioresistance. These findings emphasize the critical role of CXCR4 as a cancer stem cell marker and its potential as a therapeutic target for treating malignant chordomas.

Results

CXCR4⁺ DTC cells demonstrated a robust potential for self-renewal, tumor-initiating capacity, and resistance to IR *in vitro*

Previous studies have suggested a correlation between CXCR4 expression and CSC phenotype in various sarcomas.[11−15] However, this association remains unclear in chordomas. Our previous study found significantly higher CXCR4 expression in DTC than in U-CH1, the conventional chordoma cell line.[9] In the present study, we explored the role of CXCR4 in DTC stemness. To confirm this, we investigated whether CXCR4⁺ DTC cells are CSCs with self-renewal and tumorigenic capacity. CXCR4⁺ and CXCR4⁻ DTC cells were isolated by magnetic-activated cell sorting (Fig. S1) and tested for self-renewal capacity, tumorigenicity, and IR resistance *in vitro*. CXCR4⁺ DTC cells exhibited enhanced proliferation compared with CXCR4⁻ DTC cells (Figure 1a). Additionally, CXCR4⁺ DTC cells demonstrated a higher self-renewal capacity, as evidenced by the sphere-forming and limiting-dilution assays (Figure 1b,c). In soft-agar assays, CXCR4⁺ DTC cells displayed superior colony-forming ability, indicating an increased *in vitro* tumorigenic potential (Figure 1d). Furthermore, CXCR4⁺ DTC cells exhibited elevated resistance to IR compared with CXCR4⁻ DTC cells (Figure 1e). Western blotting and reverse transcription-PCR (RT-PCR) analyses revealed significantly higher expression of the stemness-related gene *Sox2* in CXCR4⁺ DTC cells than in CXCR4⁻ DTC cells (Figure 1f). These findings suggest that CXCR4⁺ DTC cells possess heightened stemness activity, tumorigenic potential, and IR resistance compared to their CXCR4⁻ counterparts.

CXCR4 plays a functional role in self-renewal and tumor-initiating capacity and IR resistance in DTC cells

To further examine the role of CXCR4 in DTC cells, we used short hairpin RNA targeting CXCR4 (shCXCR4) to knock down CXCR4 expression. The introduction of shCXCR4 led to reduced cell growth (Figure 2a) and suppressed the self-renewal capacity, as indicated by sphere-forming and limiting-dilution assays (Figure 2b,c). In soft-agar colony-forming assays, shCXCR4 DTC cells exhibited decreased *in vitro* tumorigenicity (Figure 2d). Additionally, these cells displayed increased sensitivity to IR upon CXCR4 knockdown (Figure 2e). Western blotting, RT-PCR, and immunofluorescence analyses demonstrated that CXCR4 knockdown down-regulated Sox2 expression and phosphorylation of STAT3, a downstream target of CXCR4 (Figure 2f,g). These results suggest that CXCR4 signaling is crucial for DTC cells' self-renewal activity, tumorigenicity, and IR resistance.

To validate the effect of CXCR4 inhibition on DTC cells, we treated cells with AMD3100, a specific CXCR4 inhibitor. In this study, we used 10 and 30 μM of AMD3100, as these are the minimal and maximal concentrations that can be effective without causing severe toxicity to the DTC cells. AMD3100 treatment resulted in a slight but significant reduction in DTC proliferation after 72 h of incubation (Fig. S2A). Additionally, AMD3100 inhibited the sphere-forming ability in a dose-dependent manner (Fig. S2B). Limiting-dilution assays showed that AMD3100-treated DTC cells had decreased self-renewal potential (Fig. S2C). In soft-agar assays, AMD3100 significantly reduced colony-forming capacity (Fig. S2D), and enhanced sensitivity to IR (Fig. S2E). Western blotting, RT-PCR, and immunofluorescence analyses confirmed reduced phosphorylation of CXCR4 and STAT3, along with decreased Sox2 expression, in response to AMD3100 treatment (Fig. S2F, G). These findings underscore the importance of CXCR4 signaling in the self-renewal activity, tumorigenicity, and IR resistance of DTC cells.

CXCR4-mediated STAT3 and Sox2 signaling is crucial for self-renewal, tumor-initiating capacity, and IR resistance in DTC cells

Next, we investigated the role of CXCR4 downstream signaling, specifically STAT3 and Sox2, in untransfected DTC cells' self-renewal activity and IR resistance. Treatment with the STAT3 inhibitor, WP1066, effectively suppressed cell growth (Figure 3a), self-renewal capacity (Figure 3b,c), *in vitro* tumorigenicity (Figure 3d), and IR resistance (Figure 3e) in these cells. Western blotting, RT-PCR, and immunofluorescence analyses confirmed inhibited phosphorylation of STAT3 and reduced Sox2 expression upon WP1066 treatment (Figure 3f,g). Treatment of WP1066 did not significantly affect CXCR4 expression in DTC cells (Figure 3f, left panel). In this study, we used 1 and 3 μM of WP1066, as these are the minimal and maximal concentrations that can be effective without causing severe toxicity to the DTC cells.

Furthermore, we investigated the functional role of Sox2, a downstream stemness factor associated with CXCR4 and STAT3 signaling, self-renewal activity, tumorigenicity, and IR resistance in DTC cells by introducing siRNA targeting Sox2. The impact of siSox2 was validated by western blotting, RT-PCR, and immunofluorescence analyses (Fig. S3A, B). siSOX2 transfection did not significantly affect STAT3 expression in DTC cells (Fig. S3A, left panel). The introduction of
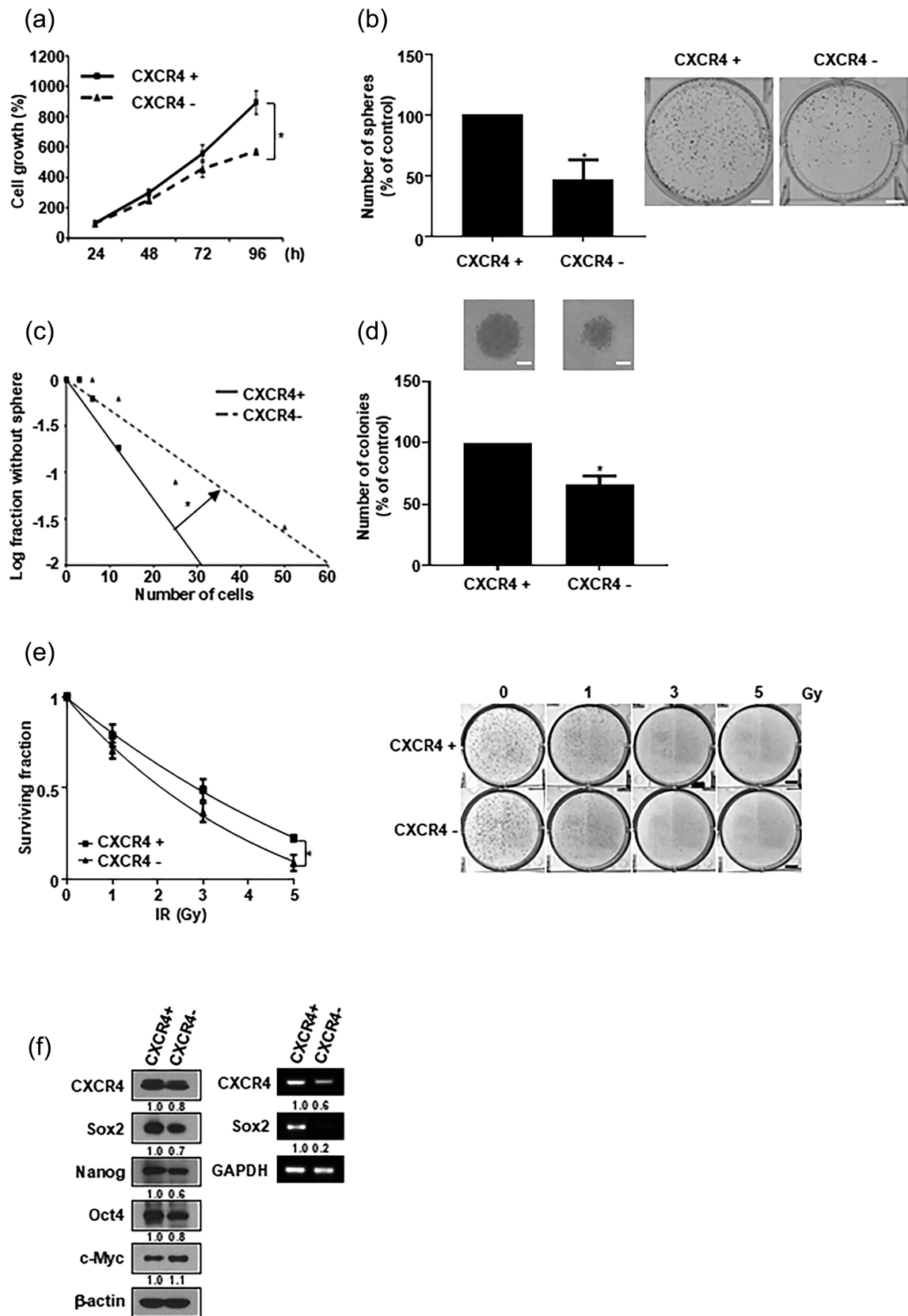
Figure 1. CXCR4+ DTC cells exhibit enhanced self-renewal activity, tumorigenic potential and IR resistance compared to CXCR4- cells. (a) MTT assay, (b) sphere-forming assay (white bar 50 mm), (c) limiting dilution assay, (d) soft agar assay (white bar 50 μm), (e) IR cl, 22onogenic survival assay (black bar 50 mm), and (f) Western blot (left) and RT-PCR (right) analyses of DTC cells after sorting with apc-conjugated CXCR4 antibody. *p < .05. All experimental results were obtained from at least three independent experiments.
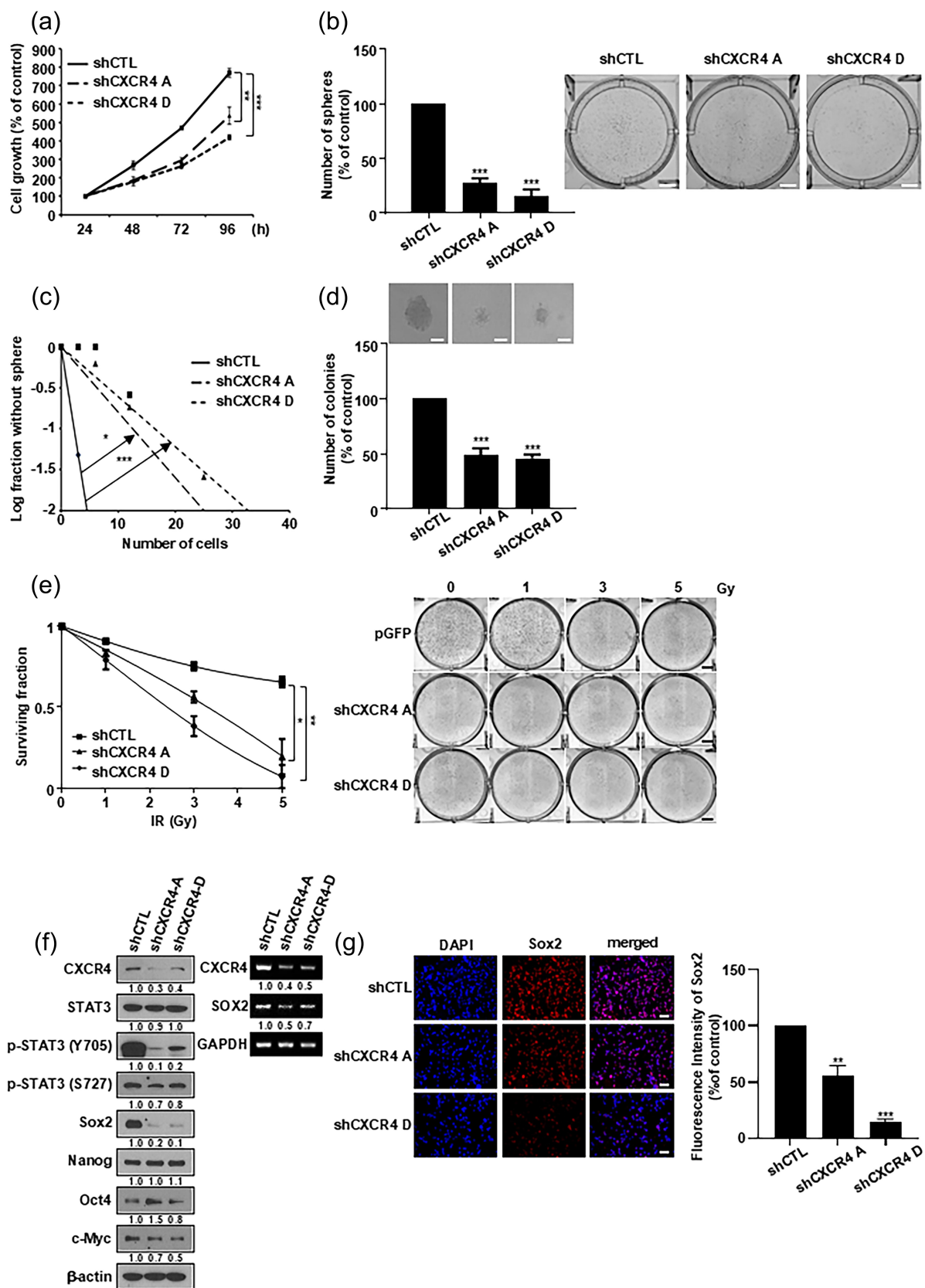
Figure 2. Silencing of CXCR4 via shRNA infection suppresses self-renewal activity, tumorigenic potential and IR resistance in DTC cells. (a) MTT assay, (b) sphere-forming assay (white bar 50 mm), (c) limiting dilution assay, (d) soft agar assay (white bar 50 μm), (e) IR clonogenic survival assay (black bar 50 mm), (f) Western blot (left) and RT-PCR (right), and (g) immunofluorescence (white bar 100 μm) analyses of DTC cells infected with shControl (shCTL), shCXCR4 a or D (upper) and quantification of the results (lower). *$p < .05$, **$p < .01$, ***$p < .001$. All experimental results were obtained from at least three independent experiments.
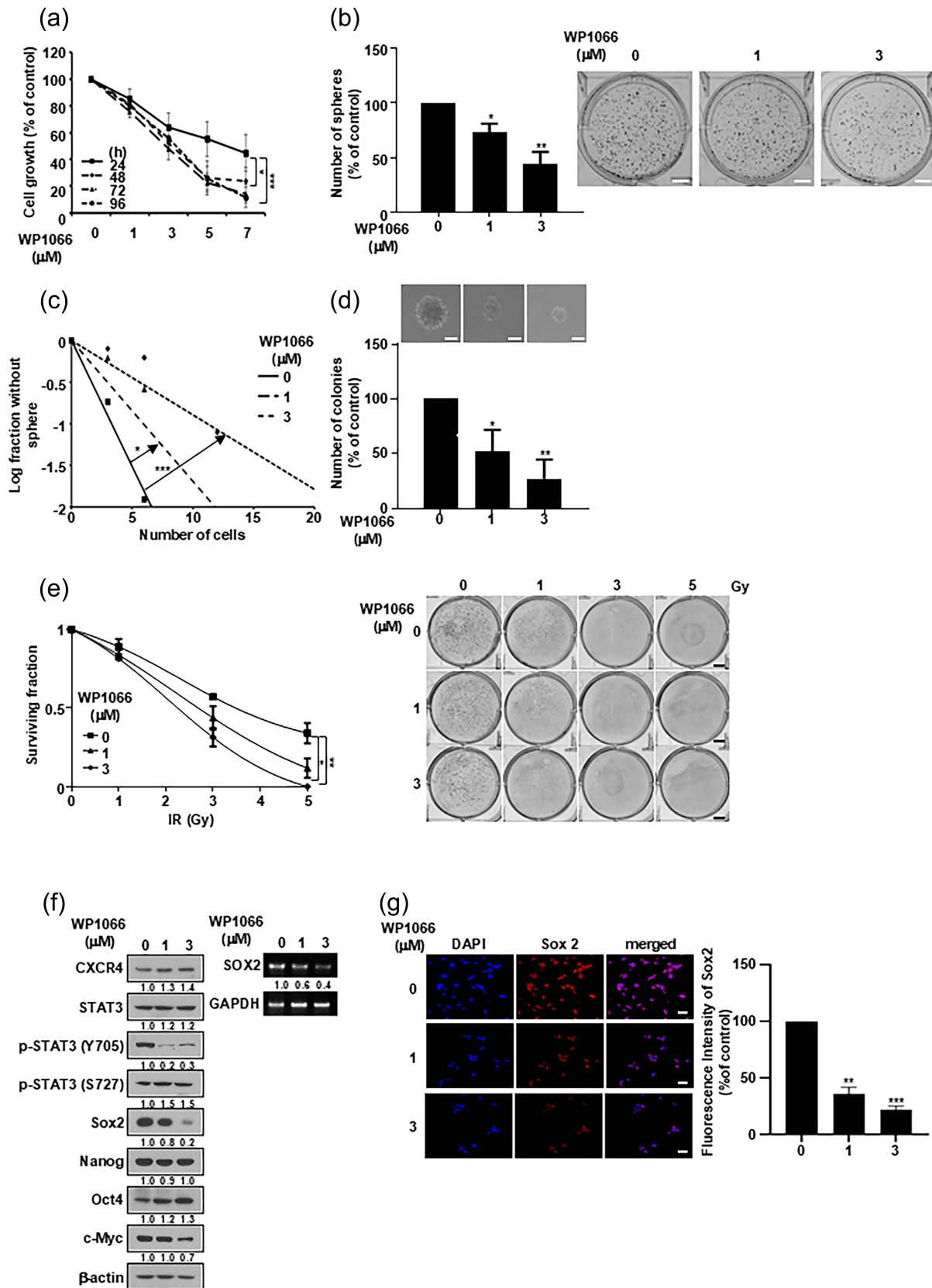
Figure 3. Pretreatment with WP1066 suppresses self-renewal activity, tumorigenic potential and IR resistance in DTC cells. (a) MTT assay, (b) sphere-forming assay (white bar 50 mm), (c) limiting dilution assay, (d) soft agar assay (white bar 50 μm), (e) IR clonogenic survival assay (black bar 50 mm), (f) Western blot (left) and RT-PCR (right), and (g) immunofluorescence (white bar 100 μm) analyses of DTC cells treated with WP1066 at the concentration indicated in the figure (upper) and quantification of the results (lower). *$p < .05$, **$p < .01$. All experimental results were obtained from at least three independent experiments.
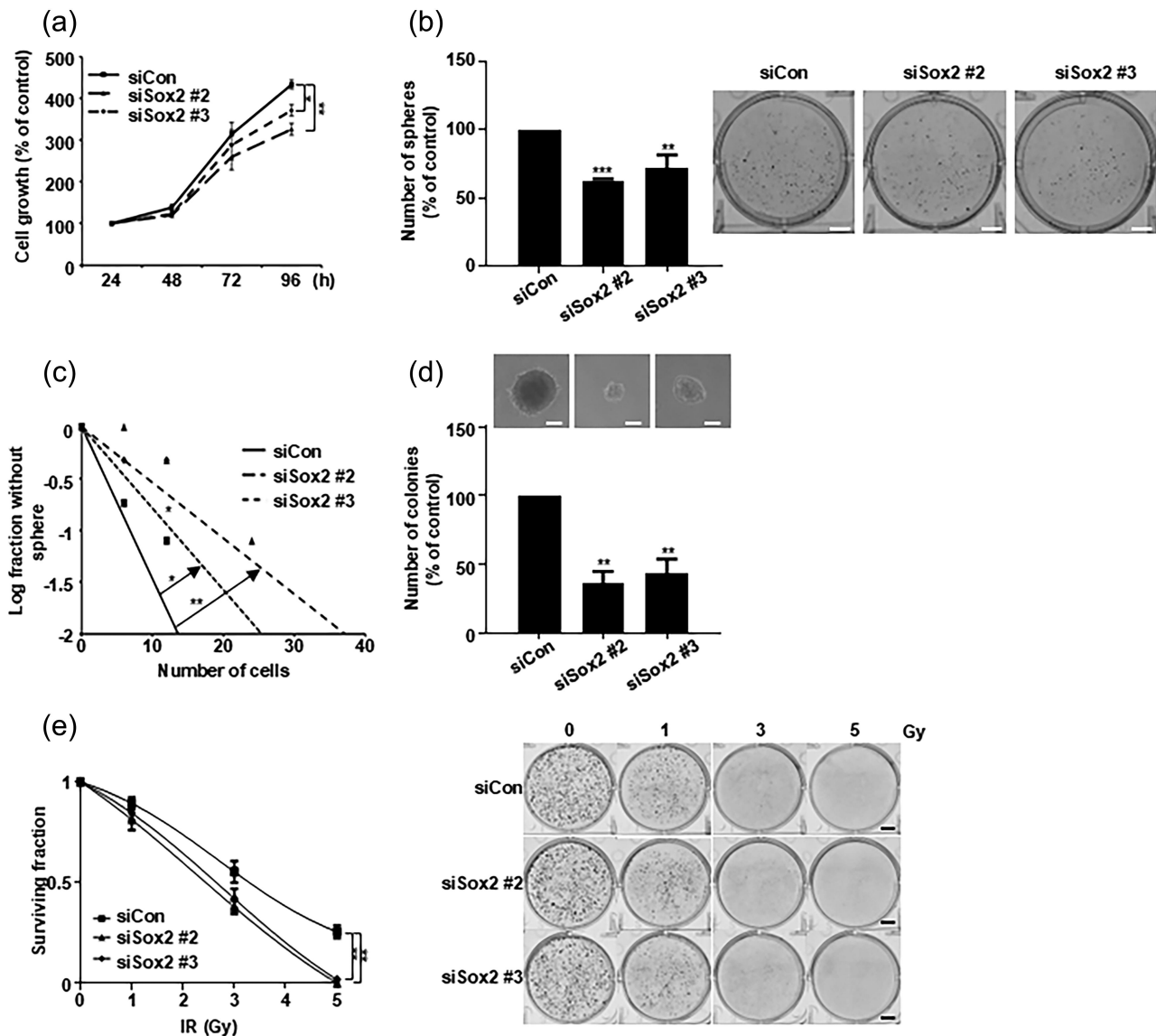
Figure 4. Silencing of Sox2 via siRNA transfection suppresses self-renewal activity, tumorigenic potential and IR resistance in DTC cells. (a) MTT assay, (b) sphere-forming assay (white bar 50 mm), (c) limiting dilution assay, (d) soft agar assay (white bar 50 μm), (e) IR clonogenic survival assay (black bar 50 mm) of DTC cells transfected with siControl (siCTL) or siSox2 #2 and #3. *$p < .05$, **$p < .01$, ***$p < .001$. All experimental results were obtained from at least three independent experiments.

siSox2 significantly impeded cell proliferation (Figure 4a) and self-renewal, as demonstrated by sphere-forming and limiting-dilution assays (Figure 4b,c). In soft-agar assays, siSox2 effectively inhibited colony formation (Figure 4d) and increased sensitivity to IR (Figure 4e). These findings underscore the crucial role of CXCR4/STAT3/Sox2 signaling in the self-renewal activity, tumorigenicity, and IR resistance of DTC cells *in vitro*.
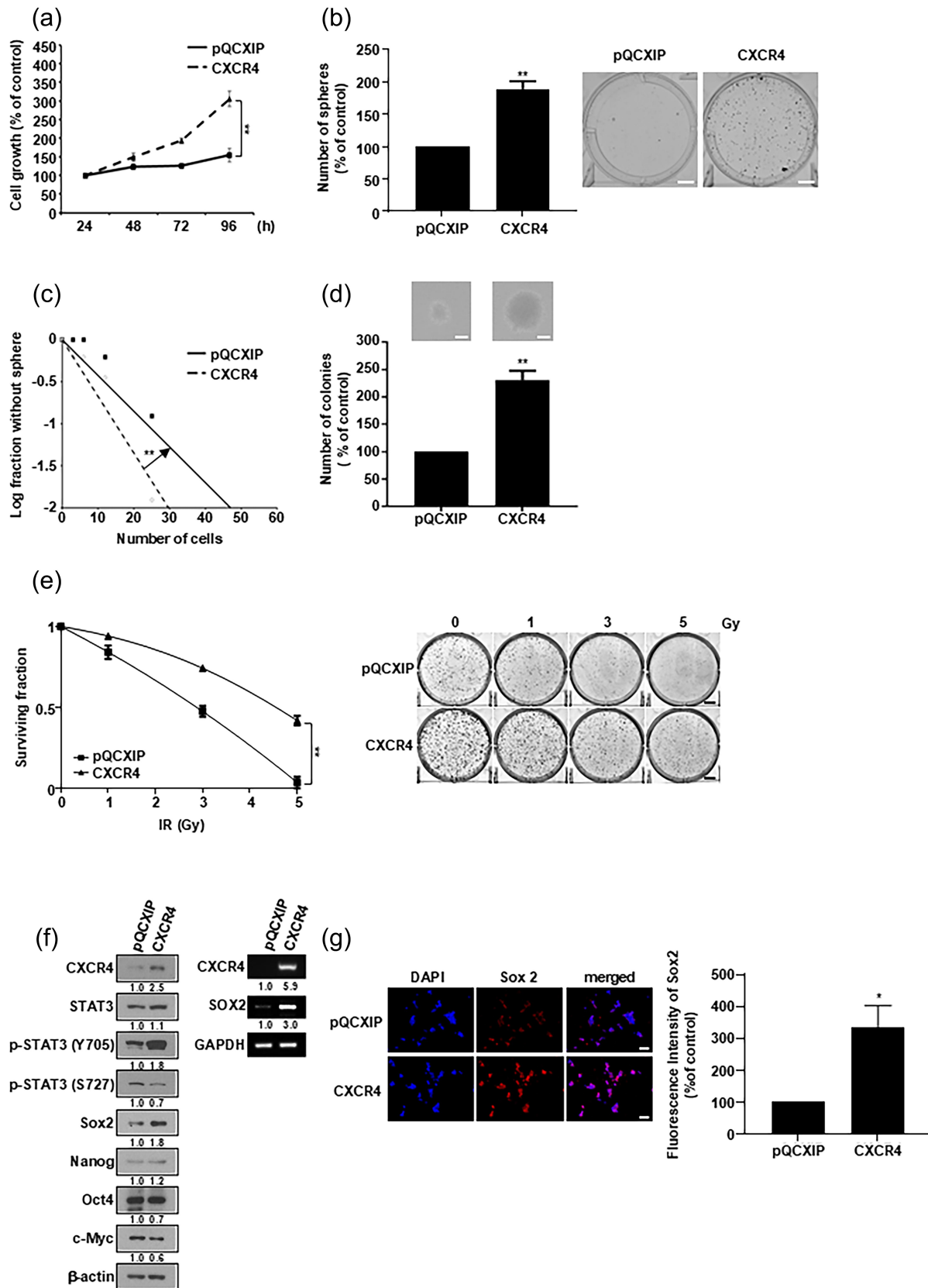
Overexpression of CXCR4 exhibited high potential for tumor-initiating capacity and IR resistance in U-CH1 cells

Additionally, we conducted gain-of-function studies using U-CH1 cells expressing low levels of CXCR4. We introduced retrovirus-mediated CXCR4 into U-CH1 cells, which enhanced cell proliferation and self-renewal (Figure 5a–c). Moreover, CXCR4 overexpression increased *in vitro*

tumorigenic potential (Figure 5d) and resistance to IR (Figure 5e). CXCR4 overexpression significantly increased phosphorylation of STAT3 and Sox2 expression in U-CH1 cells (Figure 5f,g). These findings demonstrate that CXCR4 overexpression enhances the self-renewal activity, tumorigenicity, and IR resistance of U-CH1 cells *in vitro*.

Downregulation of CXCR4 reduced tumorigenic potential, and combination therapy of IR and a CXCR4 inhibitor synergistically reduced tumor growth in the DTC xenograft model

We evaluated the effects of CXCR4 on DTC tumor growth *in vivo*. DTC cells infected with shControl or shCXCR4 were implanted into nude mice via subcutaneous injection. As depicted in Figure 6a, the tumor growth of shCXCR4-infected DTC cells was markedly suppressed compared with

Figure 5. CXCR4 overexpressing U-CH1 cells exhibited higher self-renewal activity, tumorigenic potential and IR resistance than control cells. (a) MTT assay, (b) sphere-forming assay (white bar 50 mm), (c) limiting dilution assay, (d) soft agar assay (white bar 50 μm), (e) IR clonogenic survival assay (black bar 50 mm), (f) Western blot (left) and RT-PCR (right), and (g) immunofluorescence (white bar 100 μm) analyses of DTC cells of transduced with control (pQCXIP) and CXCR4 carrying retroviruses in U-CH1 cells (upper) and quantification of the results (lower). *$p < .05$, **$p < .01$. All experimental results were obtained from at least three independent experiments.

(a)
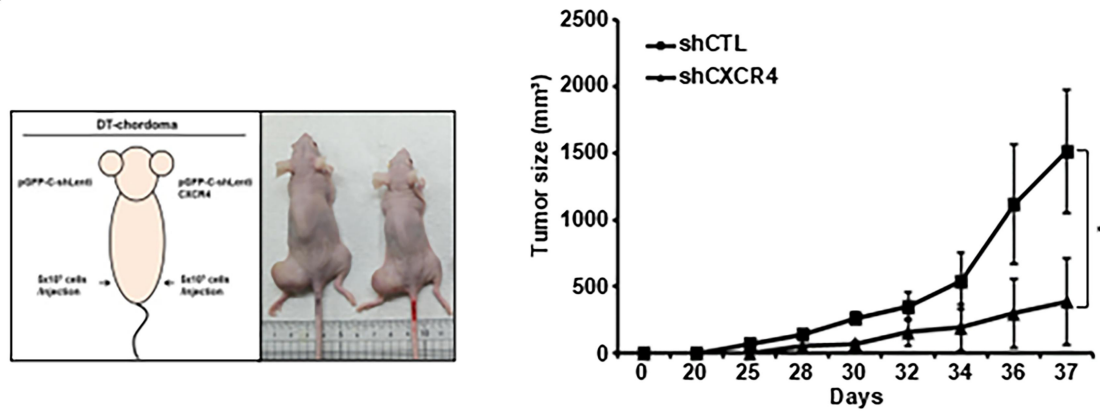
(b)
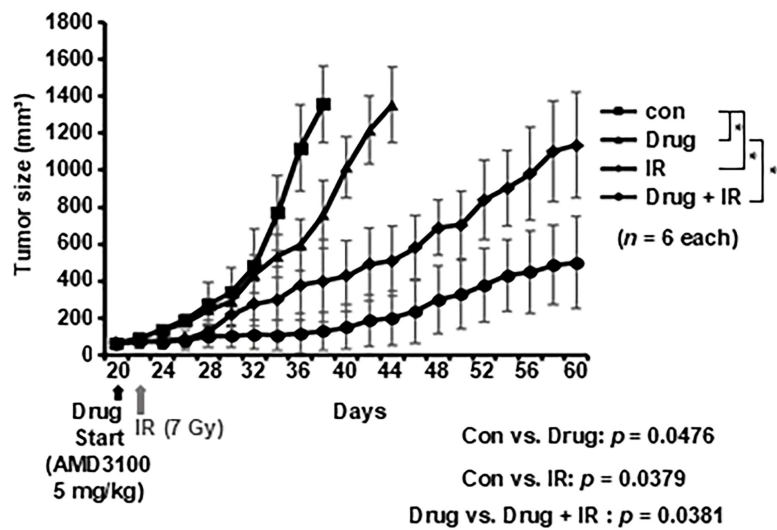
(c)
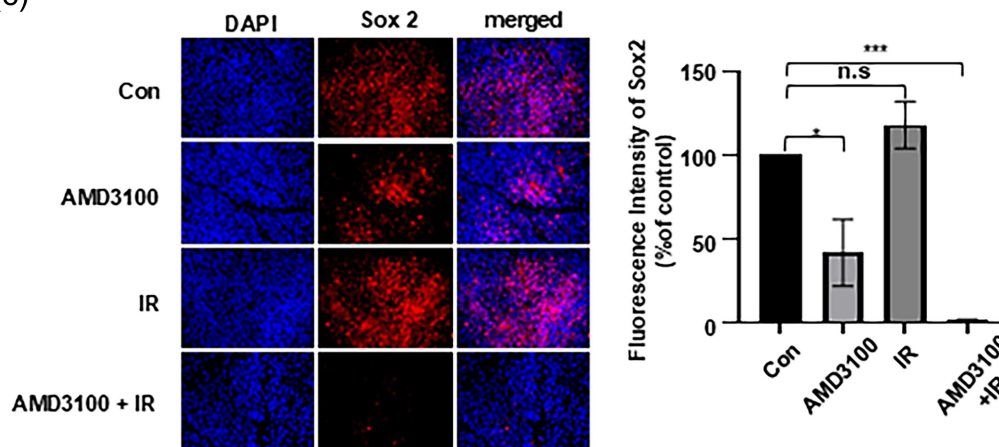
Figure 6. Suppression of CXCR4 reduced tumorigenic potential and enhanced IR sensitivity of DTC cell in an *in vivo* xenograft model. (a) A representative image of tumor-bearing mice (left) and measurement of *in vivo* tumor growth rate (right) in shControl (shCTL) and shCXCR4-infected DTC cells subcutaneously transplanted in mice. (b) Combination therapy of IR and CXCR4 inhibitor (AMD3100, 5 mg/kg) in xenograft mouse model. (c) Immunohistochemistry (white bar 50 μm) of xenograft tissues probed with Sox2 antibody (left) and quantitation of the results (right) *$p < .05$, ***$p < .001$.

that of shControl-infected DTC cells. Subsequently, we investigated the combined therapeutic effect of IR and the CXCR4 inhibitor AMD3100 in a DTC xenograft model. As shown in Figure 6b, the group treated with AMD3100 and IR exhibited a significant reduction in tumor growth. Immunohistochemical analysis revealed that AMD3100 treatment significantly suppressed Sox2 expression in xenograft tissues (Figure 6c). These findings suggest that CXCR4 plays a pivotal role in the tumorigenicity of DTC and could serve as a promising therapeutic target for enhancing IR sensitivity *in vivo*.

Discussion

Chordomas originate from embryonic notochord remnants and are challenging to treat due to the presence of chemo- and radiotherapy-resistant CSCs. Conventional therapies often prove ineffective against chordomas, necessitating innovative approaches for their treatment. CXCR4 has been recognized as a potential CSC marker in various cancers.[14–17] In primary cultured glioma cell lines, CXCR4 expression was notably higher in CD133+ cells compared to CD133-cells.[21] Similar findings were observed in prostate cancer cells, where CXCR4 + cells were enriched in CD133+ populations.[15] In addition, stimulation of CXCR4 by SDF-1α significantly induced invasion of CXCR4+ spheroid-forming breast cancer cells.[22] In our prior research, we identified the functional significance of CXCR4 in stem cell activities in drug-resistant non-small cell lung cancer cells.[16] However, the role of CXCR4 in chordoma CSC stemness remains poorly understood. This study is the first to reveal the crucial role of CXCR4 as a functional stemness factor in chordoma.

Our findings demonstrate that CXCR4+ DTC cells exhibit significantly higher self-renewal capacity, sphere-forming activity, tumorigenicity, and resistance to IR *in vitro* compared to CXCR4- DTC cells. Consistent with these results, the down regulation of CXCR4 via shCXCR4 or pharmacological inhibition of CXCR4 signaling markedly suppressed self-renewal activity, tumorigenicity, and IR resistance. Conversely, over-expression of CXCR4 reversed these effects in conventional chordoma cell line, U-CH1. Furthermore, our previous research, as indicated in reference 9, confirmed that the DTC cell line derived from recurrent cancer patients exhibited significantly higher CXCR4 expression than U-CH1. Critically, the downregulation of CXCR4 suppressed DTC tumor growth, and when combined with IR and AMD3100 treatment, it significantly enhanced therapeutic efficacy *in vivo*. These results strongly suggest that CXCR4-positive cells may represent CSCs with tumorigenic potential, highlighting the critical role of CXCR4 in the stemness and IR resistance of DTC cells.

Recent studies, including ours, have identified a significant relationship between chordoma and the chemokine receptor CXCR4. In particular, dedifferentiated chordoma cell lines have been found to exhibit high surface expression of CXCR4, which is associated with increased tumorigenic potential and the ability to form subcutaneous tumors in animal models.[9,23] This suggests that CXCR4 may contribute to the aggressiveness and metastatic behavior of chordomas. Additionally, poorly differentiated chordomas with SMARCB1/INI1 deficiency and TP53 mutations have shown upregulation of CXCR4, further implicating this receptor in tumor progression and metastasis.[24] These findings highlight the potential of CXCR4 as a therapeutic target in managing chordoma. However, Zhang et al. identified a stem-like cell cluster in skull base chordoma (SBC) marked by cathepsin L (CTSL) expression, which may contribute to radioresistance.[25] Additionally, their study highlights the significance of partial epithelial – mesenchymal transition (p-EMT) signatures in malignant cells, associating them with increased invasiveness and poor prognosis in SBC. Based on these studies, CXCR4 appears to influence stemness and aggressiveness in chordoma, specifically in certain cell types depending on their degree of differentiation.

Several studies, including our own, have linked CXCR4 to STAT3 signaling in various tumors.[16,26–30] Ligand-mediated activation of CXCR4 leads to STAT3 phosphorylation, contributing to malignancy in breast and small cell lung cancer.[27,28] It has been reported that CXCR4-mediated STAT3 activation is crucial for the invasion of bladder cancer cells.[29] Additionally, CXCR4-STAT3 signaling induces the expression of slug and VEGF in non-small cell lung cancer cells.[26,28] Although there are various effector molecules downstream of CXCR4, our previous studies identified STAT3 as a key downstream target molecule involved in CXCR4-mediated stemness and radioresistance in lung cancer cells.[16,29] Therefore, this study also focused on the impact of STAT3 on stemness and radioresistance in DTC cells. In our current study, we discovered that CXCR4-mediated STAT3 signaling plays a crucial role in maintaining the stemness of DTC cells by inducing Sox2 expression. However, the precise downstream signaling cascade for Sox2 expression in these cells needs further clarification in future studies.

The NF-κB and STAT3 signaling pathways are pivotal in regulating immune responses, inflammation, and tumorigenesis. These pathways exhibit significant crosstalk, influencing each other's activity through various mechanisms. For instance, NF-κB can induce the expression of interleukin-6 (IL-6), a cytokine that activates STAT3, thereby linking inflammatory responses to STAT3 signaling. Conversely, STAT3 can modulate NF-κB activity by regulating the expression of genes that either promote or inhibit NF-κB signaling. This bidirectional interaction facilitates a complex regulatory network that impacts cell survival, proliferation, and inflammation. Understanding the interplay between NF-κB and STAT3 is crucial, as their cooperative signaling has been implicated in the progression of various cancers, including those of the colon, stomach, and liver.[31] Although direct studies on NF-κB and STAT3 interaction in chordoma are limited, research in other cancers suggests that these pathways often cooperate to promote tumorigenesis. NF-κB and STAT3 can physically interact, co-regulate gene transcription, and enhance inflammation-driven tumor progression. Given their overlapping roles in cell survival and immune modulation, further research is needed to explore their crosstalk in chordoma.[32]

Resistance to radiation therapy is a characteristic trait of CSCs, and CXCR4 signaling is implicated in the radioresistance of malignant cancer stem cells.[7,33,34] Therefore, we

investigated whether CXCR4 has intrinsic resistance to IR in DTC cells. Our findings clearly indicated that CXCR4 knockdown or pharmacological inhibition using AMD3100 enhanced IR sensitivity in DTC cells. Conversely, CXCR4 overexpression increased IR resistance in CXCR4-low conventional-type chordoma cell line, U-CH1. Notably, the combination therapy of AMD3100 and IR synergistically reduced DTC tumor growth, suggesting that inhibiting CXCR4 signaling using AMD3100 enhances IR sensitivity. Since AMD3100 (plerixafor) was FDA approved in 2008, it could potentially be applied to enhance IR treatment efficacy in chordoma patients, making CXCR4 a promising therapeutic target for malignant chordomas.

The clinical implications of CXCR4 inhibitors have several advantages. Firstly, CXCR4 plays a crucial role in the movement and metastasis of tumor cells, and its inhibition can suppress tumor metastasis. Secondly, CXCR4 inhibition can control tumor growth by suppressing the survival and proliferation of tumor cells. Thirdly, when used in conjunction with radiation therapy or chemotherapy, CXCR4 inhibition can reduce the radioresistance of tumor cells. These advantages indicate the promising potential of CXCR4 inhibitors in cancer treatment[35,36] Therefore, the aforementioned advantages could be applied to the treatment of chordoma.

The chemokine receptor CXCR4 has been implicated in the development and progression of various cancers. Overexpression of CXCR4 is associated with increased tumor aggressiveness and poor clinical outcomes. A systematic review analyzing data from 85 studies encompassing over 11,000 patients concluded that CXCR4 expression serves as a significant and independent biomarker for worse prognosis in cancer.[37] This suggests that targeting CXCR4 could be a viable therapeutic approach. Although studies on the clinical significance of CXCR4 expression in chordoma are limited, further large-scale, multi-institutional studies using clinical samples are anticipated in the future.

Conclusions

In this study, we identified the mechanism by which CXCR4 regulates tumor-initiating capacity and radioresistance in DTC cells. Our findings suggest that targeting CXCR4 could enhance the therapeutic efficacy of chordoma, offering a novel approach to complement existing treatments. Future research should explore the clinical applicability of combining CXCR4 inhibitors with radiation therapy and further investigate the detailed mechanisms underlying CXCR4 signaling. These efforts could pave the way for a new paradigm in chordoma treatment.

Materials and methods

Materials

Antibodies against Oct4 (#sc-8628), c-Myc (#sc-40), STAT3 (#sc-482), and β-actin (#sc -47,778) were purchased from Santa Cruz Biotechnology (Dallas, TX, USA). Antibodies against Sox2 (#3579), Nanog (#4903), phosphor-STAT3 (Y705, #9145), and phosphor-STAT3 (S727, #9134) were

purchased from Cell Signaling Technology, Inc. (Danvers, MA, USA). Antibodies against CXCR4 (#ab124824) and phosphor-CXCR4 (S399, #ab74012) were purchased from Abcam (Boston, MA, USA). Specific inhibitors of CXCR4 (AMD3100, #A5602) and STAT3 (WP166, #573097) were purchased from Sigma-Aldrich (St. Louis, MO, USA).

Cell culture

The establishment of the DTC cells and their characteristics, including the expression of CXCR4 and other markers such as brachyury and cytokeratin, were described in our previous study (9). U-CH1 cells were obtained from the American Type Culture Collection (#CRL3217; Manassas, VA, USA). All cell lines were cultured in DMEM/F12 (#10–090-CVR; Cellgro, Thermo Fisher Scientific, Waltham, MA, USA) supplemented with 100 U/ml penicillin, 100 µg/ml streptomycin (#15140122; Gibco, Thermo Fisher Scientific) and 10% fetal bovine serum (FBS; #16000044, Gibco) in a humidified incubator (#MCO-20AIC; Sanyo, Osaka, Japan) with 5% CO_2 at 37°C. Primary cultured DTC cells were utilized within 10–20 passages, whereas UCH-1 cells were used within 10 passages after thawing.

Knockdown or overexpression of CXCR4

For the knockdown of CXCR expression in DTC cells, pGFP-C-shLenti and pGFP-C-shLenti CXCR4 vectors were obtained from OriGene (#TL313630; Rockville, MD, USA). Lentiviruses (2nd generation packaging system) were produced by transfecting 293T cells (#CRL3216; ATCC) with a lentivirus vector (5 µg) and packaging mix (6 µg; pMD2G, pSPAX2, and shRNA vector in a 1:2:3 ratio) using Lipofectamine^{TM} 2000 (#11668019; Invitrogen, Carlsbad, CA, USA). After 48 h of transfection, the viral supernatants were collected, filtered, concentrated using Lenti-X concentrator (#PT4421–2, Takara, Japan) and stored in a deep freezer with polybrene (8 µg/ml; #S2667; Sigma-Aldrich) until use. The cells were infected with the prepared virus stock at a multiplicity of infection of 5.

For the overexpression of CXCR4 in U-CH1 cells, the pQCXIP retroviral vector was obtained from Takara Bio, Inc. (#631516; Mountain View, CA, USA), and CXCR4 was subcloned into the vector. Retrovirus production was performed by transfecting 293T cells with viral vectors and packaging mix using Lipofectamine 2000. After 48 h of transfection, the viral supernatants were collected, filtered, and stored in a deep freezer with polybrene until use.

Transfection of small interfering RNA (siRNA)

DTC cells were transfected with siRNAs targeting Sox2. The sequences of siRNA against Sox2 (siSox2 #2 Sense 5′-AACCAAGACGCUCAUGAAGAAGGAT-3′ Antisense 5′-UUUUGGUUCUGCGAGUACUUCUUCCUA-3′; siSox2 #3 Sense 5′-AUGGACAGUUACGCGCACAUGAACG-3′ Antisense 5′-CGUACCUGUCAAUGCGCGUGUACUUGC-3′) and negative control siRNA (sense 5'-CGUUAAUCGCGUAUAAUACGCGUAT-3', Antisense 5'-

AUACGCGUAUUAUACGCGAUUAACGAC-3') were purchased from Integrated DNA Technology (Coralville, IA, USA). The siRNAs were transfected at a concentration of 20 nM using Lipofectamine™ 2000 and incubated in a humidified incubator with 5% CO_2 at 37°C. After 48 h of transfection, cells were used for the subsequent experimentations.

MTT (3-(4,5-dimethylthiazol-2-yl)-2,5-diphenyl tetrazolium bromide) assays

Cells were seeded in 96-well plates (5×10^3 cells/well) and incubated at 37°C under 5% CO_2 incubator for 24 h. The medium was replaced with 100 µl of fresh medium with or without AMD3100. After 48 h of incubation, the wells were replaced with fresh medium and MTT solution (™M5655; Sigma-Aldrich) and incubated for 2 h at 37°C incubator. After incubation, formazan was dissolved in dimethyl sulfoxide. Then, optical density was measured at 490 nm using a plate reader (iMark™ microplate absorbance reader; Bio-Rad Laboratories, Inc., Hercules, CA, USA).

Sphere-forming, limiting-dilution, soft-agar, and clonogenic survival assays

For the sphere-forming assay, a single-cell suspension obtained by trypsinization was cultured in DMEM/F12 containing 1 µl/ml B27 supplement (#17504044; Gibco), and 10 ng/ml epidermal growth factor (EGF; #AF-315-09-1 MG; Invitrogen) and 10 ng/ml primary fibroblast growth factor (FGF; #101-1B-1 MG; Invitrogen) without FBS at a density of 1×10^3 cells/ml in six-well plates (Corning, Corning, NY, USA). After 10 d, the spheres were attached by adding 10% FBS overnight, washed with phosphate-buffered saline (PBS), stained with 0.04% Crystal Violet 15 h at room temperature, and counted under an optical microscope (ECLIPSE TS100; Nikon, Tokyo, Japan).

For the limiting-dilution assay, cells were trypsinized, serially diluted, and plated in 96-well plates in 200 µl of the culture medium used for the sphere-forming assay. After 7 d of incubation, number of spheres in wells with or without spheres was counted and plotted against the number of cells per well.

To perform the soft-agar assay, single-cell suspensions (5×10^3 cells/ml) were prepared in $2 \times$ DMEM/F12 with FBS (10%) and resuspended in the same volume of 0.7% low-melting agar (final 0.35%; #A9414; Sigma-Aldrich) and poured into 24-well plates coated with agar (1:1 mixture of $2 \times$ DMEM/F12 and 1% low-melting agar; final 0.5%). After 15 d of incubation, colonies in five random fields per well were counted under an optical microscope (ECLIPSE TS100; Nikon).

For the clonogenic survival assay, a single-cell suspension obtained by trypsinization was cultured in DMEM/F12 supplemented with FBS (10% at a density of 1×10^3 cells/ml). Cells were exposed to γ-rays from a 137Cs γ-ray source (Atomic Energy of Canada, Korea Institute of Radiological and Medical Sciences) at a dose rate of 3.81 Gy/min. After 10 d, the cells were stained with 0.04% Crystal Violet overnight at room temperature and counted.

Reverse transcription-pcr (RT-PCR)

RT-PCR was performed as previously described elsewhere to quantify the endogenous mRNA expression levels. The total RNA of cells was isolated using TRIsure reagent (#BIO-38033; BIOLINE, Memphis, TN, USA) according to the manufacturer's instructions. A total of 5 µg of RNA was used to synthesize cDNA using a SensiFAST™ cDNA Synthesis kit (#BIO-65054; BIOLINE). PCR was performed using 2X MyTaqRedMix (#BIO-25043; BIOLINE) under the conditions of an annealing temperature of 60°C and 30 cycles. Oligonucleotide primer sequences used were as follows: CXCR4 forward, 5'-AATCTTCCTGCCCACCATCT-3' and reverse, 5'-GACGCCAACATAGACCACCT-3'; SOX2 forward, 5'-TGGACAGTTACGCGCACAT-3' and reverse, 5'-CGAGTAGGACATGCTGTAGGT-3'; GAPDH forward, 5'-AGGTGAAGGTCGGAGTCAAC-3' and reverse, 5'-TTCCCGTTCTCAGCCTTGAC-3'. The PCR samples underwent analysis on a 2% agarose gel, were stained with ethidium bromide (Mbiotech, Inc., Hanam, Korea), and were observed under UV light using an image analyzer (ChemiDoc XRS; Bio-Rad Laboratories, Inc., Hercules, CA, USA). To measure band density, ImageJ (NIH, USA) software was used.

Western blot analysis

Protein lysates were extracted using RIPA buffer (150 mm NaCl, 1% Triton X-100, 0.5% sodium deoxycholate, 0.1% SDS, and 50 mm Tris, pH 8.0) containing a protease inhibitor (#11697498001; Roche) and phosphatase inhibitors (#524625; Merck). The samples were incubated at 4°C for 30 min and then centrifuged at $10,000 \times g$ in a pre-chilled centrifuge at 4°C for 30 min. The supernatant was collected, and the protein concentration in the supernatant was determined using the Bradford assay (#5000006; Bio-Rad). The supernatant (20 µg) was subjected to 10% SDS-polyacrylamide gel electrophoresis and transferred onto a polyvinylidene difluoride membrane (#HATF00010; Millipore, Billerica, MA, USA). Membranes were incubated overnight at 4°C with primary antibodies. After three washes with Tris-buffered saline containing 0.1% Tween-20, the membranes were incubated with horseradish peroxidase-conjugated goat anti-rabbit (#A120-101P; Bethyl Laboratories, Inc., Montgomery, TX, USA) and goat anti-mouse (#A90-116P; Bethyl Laboratories) for 1 h at room temperature. The immunoblots were visualized using enhanced chemiluminescence (#32106; Thermo Fisher Scientific) according to the manufacturer's protocol.

Flow cytometric analysis

The cells were dissociated into single cells washed with ice-cold PBS and stained with a phycoerythrin-conjugated CXCR4 antibody (#555974; BD Biosciences, San Jose, CA, USA) in 0.1 ml of binding buffer (2% BSA and 5 mm EDTA in PBS) at a 4°C refrigerator for 1 h. After washing with ice-cold PBS

three times, the cells were resuspended in 0.1 ml of binding buffer and analyzed using MACSQuant® Analyzer10 Flow Cytometer (Miltenyi Biotec Inc; Bergisch Gladbach, Germany) and MACSQuantify™ Software 2.13 for flow cytometry analysis.

Magnetic-activated cell sorting (MACS)

To sort CXCR4$^+$ and CXCR4$^-$ cells, DTC cells were dissociated into single cells, washed with ice-cold PBS, and stained with an APC-conjugated CXCR4 antibody (#130-100-070; Miltenyi Biotec Inc., Auburn, CA, USA) in 0.1 ml of binding buffer (2% BSA and 5 mm EDTA in PBS) at a 4°C refrigerator for 1 h. After washing with ice-cold PBS three times, cells were incubated with anti-APC microbead in 0.1 ml of binding buffer at a 4°C refrigerator for 30 min. The cells were washed three times with ice-cold PBS and separated using a MACS Column (#130-042-401; Miltenyi Biotec, Inc.) placed in a MACS Separator. The flow-through fraction was collected as the negative fraction, which was depleted of labeled cells. The column was removed from the separator and the remaining cells were eluted as the enriched, CXCR4$^+$ cell fraction.

In vivo tumorigenicity study

All animal experiments were conducted following the Institutional Animal Care and Use Committee guidelines of the Korea Institute of Radiological and Medical Sciences (Ethics approval no. KIRAMS 2019–0035). BALB/c nude mice (female, 17–20 g, 6-week-old) were purchased from Orient Bio (Seongnam, Gyeonggi-do, South Korea). Cells were mixed with Matrigel (1:1, v/v; #354234; Corning, Corning, NY). Mice were anesthetized using 3% isoflurane for induction and 1.5% for maintenance, and cells were injected into the subcutaneous layer of mice. Tumor formation was checked 21–35 d after the injection. DTC tumor-bearing mice were randomized into four groups ($n = 6$). Treatments were performed with AMD3100 alone, IR alone, AMD3100 combined with IR, or control. When the tumor volume reached 100 mm^3, AMD3100 (5 mg/kg) was administered intraperitoneally, and the mice were irradiated (7 Gy) 4 days later. After IR, AMD3100 was administered daily until the completion of the experiment. Irradiation was performed using an X-ray unit operated at 260 kVp with a dose rate of 2 Gy/min (10 mA with added filtration of 2 mm copper, distance from the X-ray source to the target of 41 cm). To evaluate tumor volume, mice from all treatment groups were euthanized using CO_2 gas in the chamber (40% vol/min flow rate), and the tumor volume (mm^3) was calculated using the following formula: long diameter × (short diameter)^2 × 0.5.

Statistical analysis

Data are presented as mean ± standard deviation of three independent experiments. Differences were analyzed using Student's t-test and one-way analysis of variance (ANOVA). The results were significant at *$p < .05$, **$p < .01$, and ***p < .005. Statistical analyses and graphing were performed using Microsoft Excel 365 and GraphPad Prism 8 software (GraphPad Software).

ORCID

Myung-Jin Park 🆔 http://orcid.org/0000-0002-1996-4083

Author's contributions

C-WJ and J-YK performed experiments; J-YK analyzed the data; M-JP designed the experiments and wrote the manuscript. All authors read, reviewed and approved the final manuscript.

Data availability statement

The datasets used during the present study are available from the corresponding author upon reasonable request.

References

1. Healey JH, Lane JM. Chordoma: a critical review of diagnosis and treatment. Orthop Clin N Am. 1989;20(3):417–426.
2. McMaster ML, Goldstein AM, Bromley CM, Ishibe N, Parry DM. Chordoma: incidence and survival patterns in the United States, 1973–1995. Cancer Causes Control. 2001;12(1):1–11. doi:10.1023/A:1008947301735.
3. Yamaguchi T, Yamato M, Saotome K. First histologically confirmed case of a classic chordoma arising in a precursor benign notochordal lesion: differential diagnosis of benign and malignant notochordal lesions. Skeletal Radiol. 2002;31(7):413–418. doi:10.1007/s00256-002-0514-z.
4. Stacchiotti S, Sommer J. Chordoma global consensus group. Building a global consensus approach to chordoma: a position paper from the medical and patient community. Lancet Oncol. 2015;16(2):e71–83. doi:10.1016/S1470-2045(14)71190-8.
5. Walcott BP, Nahed BV, Mohyeldin A, Coumans JV, Kahle KT, Mj F. Chordoma: current concepts, management, and future directions. Lancet Oncol. 2012;13(2):e69–76. doi:10.1016/S1470-2045(11)70337-0.
6. Jordan CT, Guzman ML, Noble M. Cancer stem cells. N Engl J Med. 2006;355(12):1253–1261. doi:10.1056/NEJMra061808.
7. Gilbert CA, Ross AH. Cancer stem cells: cell culture, markers, and targets for new therapies. J Cell Biochem. 2009;108(5):1031–1038. doi:10.1002/jcb.22350.
8. Aydemir E, Bayrak OF, Sahin F, Atalay B, Kose GT, Ozen M, Sevli S, Dalan AB, Yalvac ME, Dogruluk T, et al. Characterization of cancer stem-like cells in chordoma. J Neurosurg. 2012;116(4):810–820. doi:10.3171/2011.12.JNS11430.
9. Kim JY, Lee JS, Koh JS, Park MJ, Chang UK. Establishment and characterization of a chordoma cell line from the tissue of a patient with dedifferentiated-type chordoma. J Neurosurg Spine. 2016;25 (5):626–635. doi:10.3171/2016.3.SPINE151077.

10. Furusato B, Mohamed A, Uhlén M, Rhim JS. CXCR4 and cancer. Pathol Int. 2010;60(7):497–505. doi:10.1111/j.1440-1827.2010.02548.x.

11. Zou YR, Kottmann AH, Kuroda M, Taniuchi I, Littman DR. Function of the chemokine receptor CXCR4 in haematopoiesis and in cerebellar development. Nature. 1998;393(6685):595–599. doi:10.1038/31269.

12. Muller A, Homey B, Soto H, Ge N, Catron D, Buchanan ME, McClanahan T, Murphy E, Yuan W, Wagner SN, et al. Involvement of chemokine receptors in breast cancer metastasis. Nature. 2001;410(6824):50–56. doi:10.1038/35065016.

13. Sun YX, Wang J, Shelburne CE, Lopatin DE, Chinnaiyan AM, Rubin MA, Pienta KJ, Taichman RS. Expression of CXCR4 and CXCL12 (SDF-1) in human prostate cancers (PCa) in vivo. J Cell Biochem. 2003;89(3):462–473. doi:10.1002/jcb.10522.

14. Ehtesham M, Mapara KY, Stevenson CB, Thompson RC. CXCR4 mediates the proliferation of glioblastoma progenitor cells. Cancer Lett. 2009;274(2):305–312. doi:10.1016/j.canlet.2008.09.034.

15. Miki J, Furusato B, Li H, Gu Y, Takahashi H, Egawa S, Sesterhenn IA, McLeod DG, Srivastava S, Rhim JS. Identification of putative stem cell markers, CD133 and CXCR4, in hTERT–immortalized primary nonmalignant and malignant tumor-derived human prostate epithelial cell lines and in prostate cancer specimens. Cancer Res. 2007;67(7):3153–3161. doi:10.1158/0008-5472.CAN-06-4429.

16. Jung MJ, Kim YM, Jung JE, Jin YB, Ko YG, Lee JS, Lee J-S, Lee S-J, Lee JC, Park M-J. Upregulation of CXCR4 is functionally crucial for maintenance of stemness in drug-resistant non-small cell lung cancer cells. Oncogene. 2013;32(2):209–221. doi:10.1038/onc.2012.37.

17. Jiang C, Ma S, Hu R, Wang X, Li M, Tian F, Jiang W, Zhu L, Bian Z. Effect of CXCR4 on apoptosis in osteosarcoma cells via the PI3K/AKT/NF-κβ signaling pathway. Cell Physiol Biochem. 2018;46(6):2250–2260. doi:10.1159/000489593.

18. Kimura T, Wang L, Tabu K, Tsuda M, Tanino M, Maekawa A, Nishihara H, Hiraga H, Taga T, Oda Y, et al. Identification and analysis of CXCR4-positive synovial sarcoma-initiating cells. Oncogene. 2016;35(30):3932–3943. doi:10.1038/onc.2015.461.

19. Ciccarelli C, Vulcano F, Milazzo L, Gravina GL, Marampon F, Macioce G, Giampaolo A, Tombolini V, Di Paolo V, Hassan HJ, et al. Key role of MEK/ERK pathway in sustaining tumorigenicity and in vitro radioresistance of embryonal rhabdomyosarcoma stem-like cell population. Mol Cancer. 2016;15(1):16. doi:10.1186/s12943-016-0501-y.

20. Oda Y, Tateishi N, Matono H, Matsuura S, Yamamoto H, Tamiya S, Yokoyama R, Matsuda S, Iwamoto Y, Tsuneyoshi M. Chemokine receptor CXCR4 expression is correlated with VEGF expression and poor survival in soft-tissue sarcoma. Intl J Cancer. 2009;124(8):1852–1859. doi:10.1002/ijc.24128.

21. Liu G, Yuan X, Zeng Z, Tunici P, Ng H, Abdulkadir IR, Lu L, Irvin D, Black KL, Yu JS. Analysis of gene expression and chemoresistance of CD133+ cancer stem cells in glioblastoma. Mol Cancer. 2006;5(1):67. doi:10.1186/1476-4598-5-67.

22. Krohn A, Song YH, Muehlberg F, Droll L, Beckmann C, Alt E. CXCR4 receptor positive spheroid forming cells are responsible for tumor invasion in vitro. Cancer Lett. 2009;280(1):65–71. doi:10.1016/j.canlet.2009.02.005.

23. Zhao C, Tan T, Zhang E, Wang T, Gong H, Jia Q, Liu T, Yang X, Zhao J, Wu Z, et al. A chronicle review of new techniques that facilitate the understanding and development of optimal individualized therapeutic strategies for chordoma. Front Oncol. 2022;12:1029670. doi:10.3389/fonc.2022.1029670.

24. Murzabdillaeva A, Elzamly S, Brown R, Buryanek J, Jafri S, Rowe J. Prometastatic CXCR4 and histone methyltransferase EZH2 are upregulated in SMARCB1/INI1-deficient and TP53-mutated metastatic poorly differentiated chordoma to the liver. Am J Clin Pathol. 2020;154(Supplement_1):S151–S151. doi:10.1093/ajcp/aqaa161.330.

25. Zhang Q, Fei L, Han R, Huang R, Wang Y, Chen H, Yao B, Qiao N, Wang Z, Ma Z, et al. Single-cell transcriptome reveals cellular hierarchies and guides p-emt-targeted trial in skull base chordoma. Cell Discov. 2022;8(1):94. doi:10.1038/s41421-022-00459-2.

26. Kim JY, Kim HJ, Jung CW, Lee TS, Kim EH, Park MJ. CXCR4 uses STAT3-mediated slug expression to maintain radioresistance of non-small cell lung cancer cells: emerges as a potential prognostic biomarker for lung cancer. Cell Death Dis. 2021;12(1):48. doi:10.1038/s41419-020-03280-5.

27. Liu X, Xiao Q, Bai X, Yu Z, Sun M, Zhao H, Mi X, Wang E, Yao W, Jin F, et al. Activation of STAT3 is involved in malignancy mediated by CXCL12-CXCR4 signaling in human breast cancer. Oncol Rep. 2014;32(6):2760–2768. doi:10.3892/or.2014.3536.

28. Wang M, Chen GY, Song HT, Hong X, Yang ZY, Sui GJ. Significance of CXCR4, phosphorylated STAT3 and VEGF-A expression in resected non-small cell lung cancer. Exp Ther Med. 2011;2(3):517–522. doi:10.3892/etm.2011.235.

29. Shen HB, Gu ZQ, Jian K, Qi J. CXCR4-mediated Stat3 activation is essential for CXCL12-induced cell invasion in bladder cancer. Tumor Biol. 2013;34(3):1839–1845. doi:10.1007/s13277-013-0725-z.

30. Pfeiffer M, Hartmann TN, Leick M, Catusse J, Schmitt-Graeff A, Burger M. Alternative implication of CXCR4 in JAK2/STAT3 activation in small cell lung cancer. Br J Cancer. 2009;100 (12):1949–1956. doi:10.1038/sj.bjc.6605068.

31. Grivennikov S, Karin M. Dangerous liaisons: STAT3 and nf-κB collaboration and crosstalk in cancer. Cytokine Growth Factor Rev. 2010;21(1):11–19. doi:10.1016/j.cytogfr.2009.11.005.

32. Krajka-Kuźniak V, Belka M, Papierska K. Targeting STAT3 and nf-κB signaling pathways in cancer prevention and treatment: the role of Chalcones. Cancers. 2024;16(6):1092. doi:10.3390/cancers16061092.

33. Trautmann F, Cojoc M, Kurth I, Melin N, Bouchez LC, Dubrovska A, Peitzsch C. CXCR4 as biomarker for radioresistant cancer stem cells. Int J Radiat Biol. 2014;90(8):687–699. doi:10.3109/09553002.2014.906766.

34. Goffart N, Lombard A, Lallemand F, Kroonen J, Nassen J, Di Valentin E, Berendsen S, Dedobbeleer M, Willems E, Robe P, et al. CXCL12 mediates glioblastoma resistance to radiotherapy in the subventricular zone. Neuro Oncol. 2017;19(1):66–77. doi:10.1093/neuonc/now136.

35. Teicher BA, Fricker SP. CXCL12 (SDF-1)/CXCR4 pathway in cancer. Clin Cancer Res. 2010;16(11):2927–2931. doi:10.1158/1078-0432.CCR-09-2329.

36. Domanska UM, Kruizinga RC, Nagengast WB, Timmer-Bosscha H, Huls G, de Vries EG, Walenkamp AME. A review on CXCR4/CXCL12 axis in oncology: no place to hide. Eur J Cancer. 2013;49 (1):219–230. doi:10.1016/j.ejca.2012.05.005.

37. Zhao H, Gupo L, Zhao H, Zhao J, Weng H, Zhao B. CXCR4 over-expression and survival in cancer: a system review and meta-analysis. Oncotarget. 2015;6(7):5022–5040. doi:10.18632/oncotarget.3217.